Electrochimica Acta 56 (2011) 8534–8538

Contents lists available at ScienceDirect

Electrochimica Acta

journal homepage: www.elsevier.com/locate/electacta

Low-temperature growth of well-crystalline Co_3O_4 hexagonal nanodisks as anode material for lithium-ion batteries

S.W. Hwang[a], Ahmad Umar[a,*], S.H. Kim[a], S.A. Al-Sayari[a], M. Abaker[a], A. Al-Hajry[a], A. Manuel Stephan[b]

[a] Collaborative Research Centre for Sensors and Electronic Devices (CRCSED) and Centre for Advanced Materials and Nano-Engineering (CAMNE), Najran University, P.O. Box 1988, Najran 11001, Saudi Arabia
[b] Electrochemical Power Systems Division, Central Electrochemical Research Institute, Karaikudi 630 006, India

ARTICLE INFO

Article history:
Received 8 April 2011
Received in revised form 9 July 2011
Accepted 11 July 2011
Available online 20 July 2011

Keywords:
Co_3O_4 hexagonal nanodisks
Anode material
Li-ion batteries

ABSTRACT

Uniform hexagonal-shaped cobalt oxide (Co_3O_4) nanodisks were prepared in large scale via facile aqueous solution based hydrothermal process at 110 °C. The detailed structural characterizations confirmed that the synthesized products are hexagonal cobalt oxide nanodisks, possessing very well-crystalline cubic spinel structure. A coin cell of type −2032 was assembled using the synthesized Co_3O_4 nanodisks and its charge–discharge profile was analyzed between the voltages 0.01 and to 2.5 V *vs.* Li/Li^+ reference electrode. The electrochemical cell composed of Li/Co_3O_4 delivered an initial lithium insertion capacity of 2039 mAh/g. Although the cell exhibited high irreversible capacity during the first four cycles, the columbic efficiency has been improved upon cycling.

1. Introduction

The rechargeable lithium ion batteries are one of the most important portable power sources for a variety of electronic devices such as laptop computers, mobile phones, power supply to hybrid electric vehicles (HEVs) and electric vehicles, etc. [1–5]. In this regard, the development of new electrode materials (anode and cathode) for Li-ion batteries is one of the main research focuses. Therefore, significant efforts have been made to design new electrode materials to improve the energy and power capability of batteries [1–5]. The carbon/graphite-related materials have been the most applied anodes in small size secondary lithium-ion batteries [3,4]. Additionally, various metals with high theoretical capacity such as Si, Sn, Ge, Al, and Sb have also been explored as anode material [6–9]. Recently, transition metal oxides such as SnO_2, TiO_2, MoO_3, Fe_2O_3, and Co_3O_4 have also been used as anode materials for Li-ion battery applications [1]. Due to larger surface area and spatial confinement effect, the nanomaterials possess considerable kinetic advantages for Li-ion battery applications and offer additional reactive sites for lithium ions to enhance specific capacity, and can shorten the path lengths to facilitate electronic and lithium ion transport which results good rate capability [1]. Among various metal oxides, cobalt oxides (Co_3O_4) is an important and interesting p-type magnetic semiconductor and has been utilized in a variety of applications such as sensors, heterogeneous catalysts, and electrochromic devices [1]. In addition to this, as Co_3O_4 exhibits excellent electrochemical performance hence variety of Co_3O_4 nanostructures have been synthesized and utilized as an anode material for Li-ion battery applications [10–13]. Wang et al. prepared thin films of nanocrystalline Co_3O_4, by reactive pulsed laser deposition (PLD) and used for Li-ion battery applications [10]. Li et al. demonstrated the utilization of Co_3O_4 nanotubes, nanorods, and nanoparticles as anode materials of Li-ion batteries [11]. Liu et al. presented that hydrothermally synthesized Co_3O_4 microspheres can efficiently be used as anode material [12]. Macroporous Co_3O_4 platelets were also utilized as anode material and reported [13].

In this paper, we report the low-temperature synthesis of well-crystalline Co_3O_4 hexagonal nanodisks and their utilization, *for the first time*, as an anode material for lithium-ion battery application. The Li-ion battery performances of as-synthesized nanodisks were studied by charge/discharge process.

2. Experimental details

In a typical reaction process, for the synthesis of Co_3O_4 hexagonal nanodisks, 1.3 g cobalt nitrate hexahydrate ($Co(NO_3)_2{\cdot}6H_2O$), dissolved in 100 ml DI water, was mixed with 0.6 g of hexamethylenetetramine (HMTA), dissolved in 100 ml DI water, under continuous stirring. Few drops of NaOH solution were added in the resultant solution to maintain the pH 10. After maintaining the pH, the resultant solution was vigorously stirred for 2 h. Consequently, the resultant solution was then loaded into a Teflon-lined stainless steel autoclave, sealed it and heated up to 110 °C for 15–24 h. After

* Corresponding author. Tel.: +966 534574597; fax: +966 75442135.
E-mail address: ahmadumar786@gmail.com (A. Umar).

0013-4686/$ – see front matter © 2011 Elsevier Ltd. All rights reserved.
doi:10.1016/j.electacta.2011.07.033

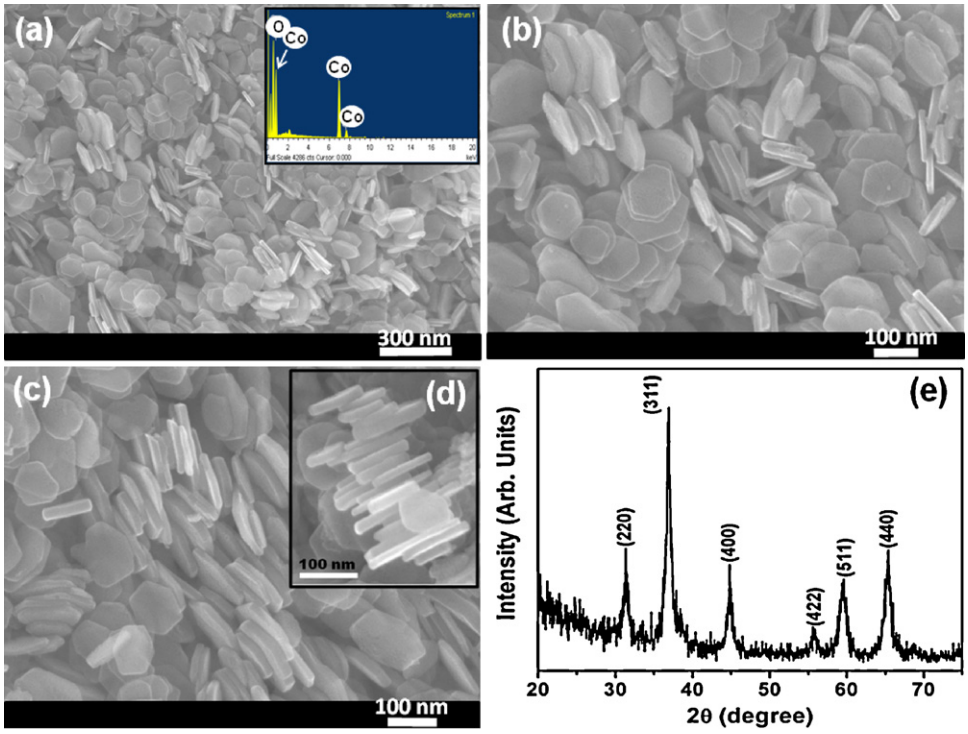

Fig. 1. Typical (a–d) FESEM images; (e) X-ray diffraction pattern and (inset (a)) corresponding EDS spectrum of the synthesized hexagonal-shaped Co_3O_4 nanodisks synthesized by facile aqueous solution based hydrothermal process.

completing the reaction in desired time, the autoclave was naturally allowed to cool at room-temperature and obtained products were washed with DI water, ethanol and acetone sequentially and dried at room-temperature. The dried products were then calcined at 200 °C for 2 h. The synthesized products were investigated in terms of their morphological, structural and compositional properties.

The general morphologies of synthesized Co_3O_4 hexagonal nanodisks were examined by FESEM (JEOL-JSM-7600F) attached with energy dispersive spectroscopy (EDS) and transmission electron microscopy (TEM; JEOL-JEM-2100F) equipped with high-resolution TEM (HRTEM). The crystallinity and crystal phases were characterized by X-ray diffraction (XRD; PANanalytical Xpert Pro.) pattern measured with Cu-Kα radiation (λ = 1.54178 Å) in the range of 20–75°. The composition of prepared Co_3O_4 products was examined by Fourier transform infrared (FTIR; Perkin Elmer-FTIR Spectrum-100) spectroscopy in the range of 500–2850 cm^{-1}.

For application point of view, the prepared Co_3O_4 hexagonal nanodisks were used as an anode material for Li-ion battery applications. To prepare the Li-ion battery anode using synthesized Co_3O_4 hexagonal nanodisks, 20 mg of synthesized nanodisks were mixed well with 13 mg of Tefronized acetylene black (TAB; it was used as binder) in the presence of few drops of Isopropyl alcohol (IPA). The prepared mixture was put on stainless steel mesh and pressed to fabricate the electrode. The made electrode was then dried in vacuum oven for 12 h at 100 °C. For preparing the coin cell using the prepared sample, the coin cell components (2032), obtained from Hosen Co. were used. The utilized electrolyte was 1 M $LiPF_6$ EC/DMC (1:1 wt%). The charge/discharge capacity measurements of the fabricated anode were performed using charge/discharge equipment (BTS200 4W, Japan). The cell was cycled between 0.01 and 2.5 V *vs.* Li/Li^+ at current density of 0.2 mA/g.

3. Results and discussion

The general morphologies of as-synthesized Co_3O_4 hexagonal nanodisks were observed by field emission scanning electron microscopy (FESEM) and demonstrated in Fig. 1(a–c). From the obtained FESEM micrographs, it is clear that the synthesized products are hexagonal nanodisks which are formed in large-quantity. The growth densities of the nanodisks are very high as even most of the nanodisks are attached with each other through one of their surfaces and exhibiting sharp edges with smooth and clean surfaces. Most of the nanodisks exhibit a perfectly hexagonal shape with an internal angle of ~120°, however some deformed hexagonal structured nanodisks were also seen in the micrographs. The nanodisks are about 100 ± 10 nm in diagonal and distributed randomly. The typical thicknesses of the nanodisks are in the range of 12 ± 3 nm (Fig. 1(d)). The composition of the synthesized nanodisks were examined by energy dispersive spectroscopy (EDS) and shown in the inset of Fig. 1(a). As can be seen from the EDS spectrum, the synthesized nanodisks are made by Co and O. The crystallinity and crystal phases of the nanodisks were examined by powder X-ray diffraction. All the obtained reflections in the pattern are well matched with the cubic spinel structure of Co_3O_4 (JCPDS Card No. 42-1467, Co_3O_4). No other reflection related with any impurity was detected in the pattern, up to the detection limit of X-ray which confirms the high purity of the synthesized nanodisks. In addition to this, obtained XRD pattern exhibits sharp reflections which could be correlated with good crystallinity of the synthesized nanodisks (Fig. 1(e)). For the detailed structural and compositional characterizations, the synthesized nanodisks were examined by transmission electron microscopy (TEM) and Fourier transform infrared (FTIR) spectroscopy and shown in Fig. 2.

Fig. 2(a and b) exhibits the low-resolution TEM images of synthesized Co_3O_4 hexagonal nanodisks which show full consistency with the observed FESEM results. Fig. 2(a) confirms that the nan-

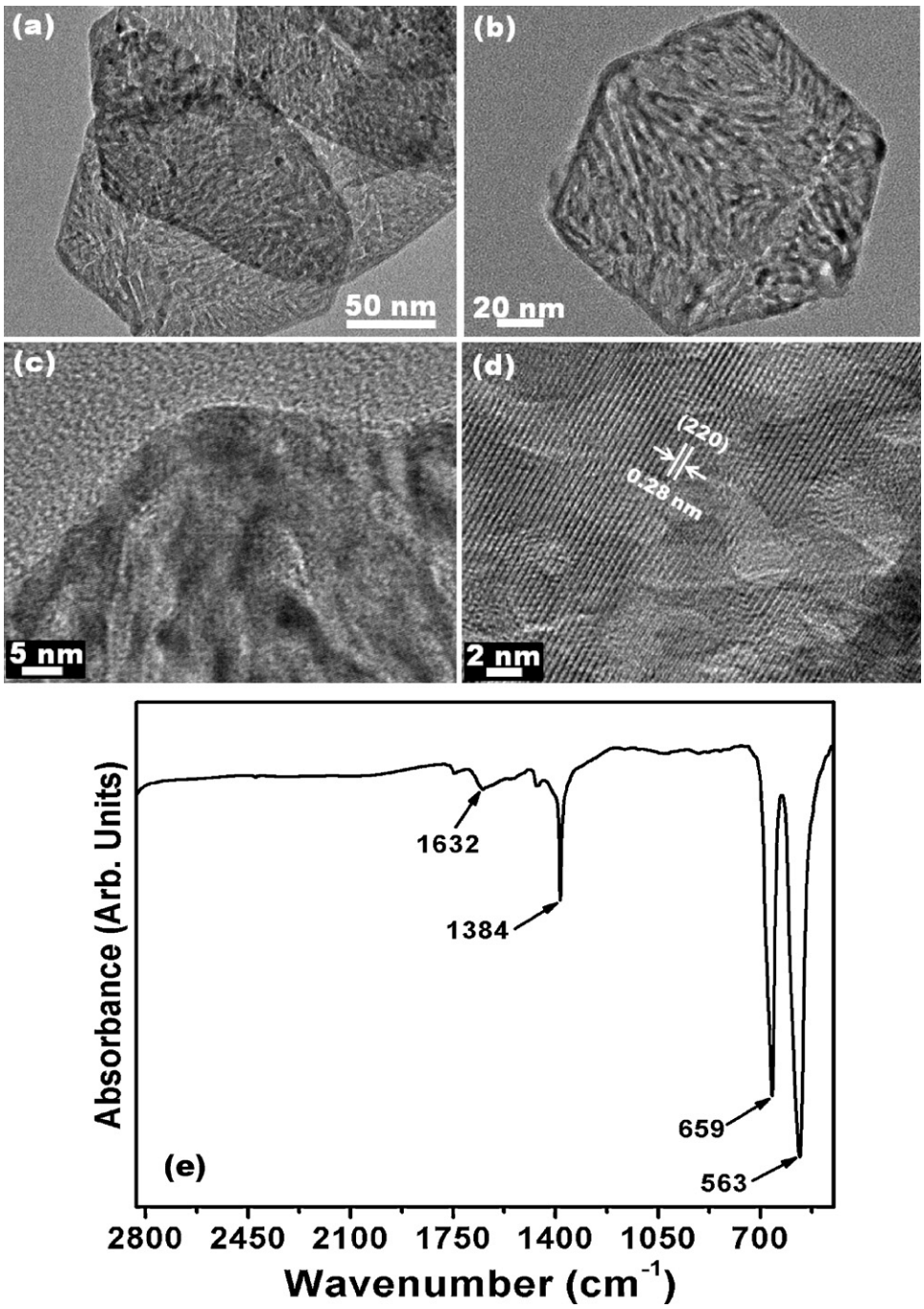

Fig. 2. Typical (a and b) low-magnification and (c and d) high-resolution TEM images; and (e) FTIR spectrum of the synthesized hexagonal-shaped Co_3O_4 nanodisks synthesized by facile aqueous solution based hydrothermal process.

odisks are grown in very high density and due to this many nanodisks are just overlap with each other. Due to very low thickness of the synthesized nanodisks, it exhibits almost transparent characteristics and their edges are overlapped that can be seen clearly. Even though having different diagonals, but interestingly, it is seen that all the nanodisks exhibit a perfectly hexagonal shape (Fig. 2(a)). Fig. 2(b) exhibits a single Co_3O_4 hexagonal nanodisk. As can be seen from the micrographs that the synthesized nanodisk is exhibiting perfectly hexagonal shape with internal angle of $\sim 120^\circ$ and diagonal of the nanodisk is $\sim 100 \pm 10$ nm. Fig. 2(c and d) demonstrates the typical high-resolution TEM image which exhibits clear and well-defined lattice fringes of the synthesized nanodisk. The measured spacing between two lattice fringes are 0.28 nm which corresponds to the (2 2 0) plane of cubic Co_3O_4 (Fig. 2(d)). The well-defined lattice fringes again confirmed that the synthesized nanodisks possessing well-crystalline structures.

Fig. 2(e) shows the FTIR spectrum of synthesized Co_3O_4 hexagonal nanodisks. Various well-defined absorption bands have been observed in the FTIR spectrum. The presence of two distinct bands at 563 and 659 cm^{-1} are due to ν_1 and ν_2 stretching vibrations of metal–oxygen bonds which confirm the formation of cubic Co_3O_4 spinel oxide. The ν_1 band is related with Co^{3+} vibration in the octahedral hole while the ν_2 band is the characteristics of Co^{2+} vibrations in tetrahedral hole in the spinel lattice [14,15]. In addition to this, an absorption band appeared at 1384 cm^{-1} was originated due to the presence of CO_3^{2-}. This band generally

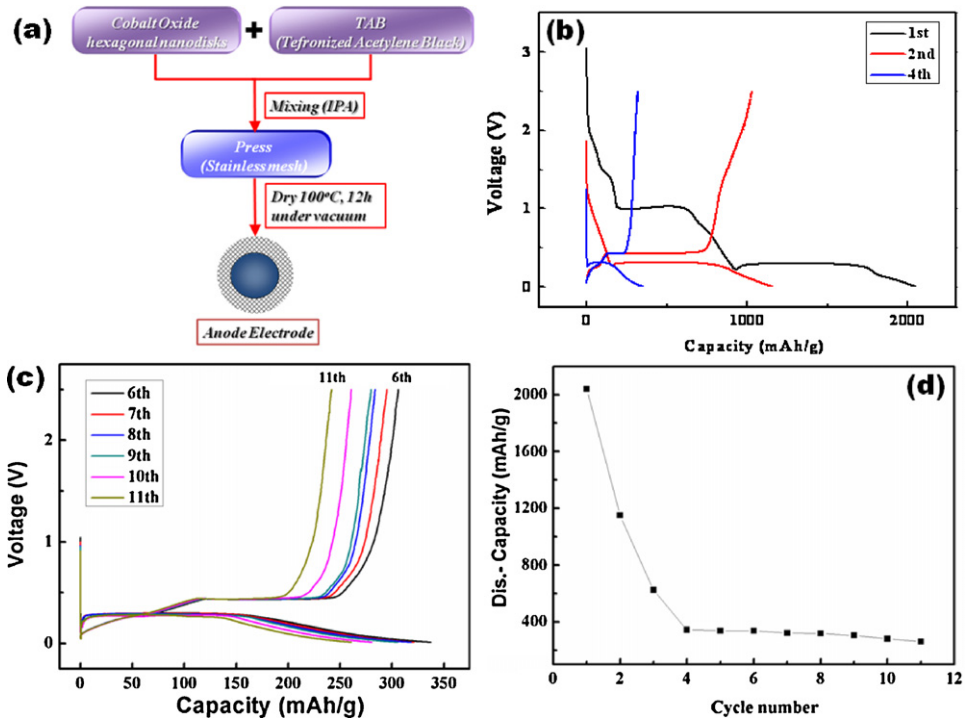

Fig. 3. (a) Typical step-by-step Li-ion battery anode fabrication process using synthesized Co_3O_4 hexagonal nanodisks. (b) Initial four cycles and (c) after 6th cycles, the charge/discharge profiles of hexagonal-shaped Co_3O_4 nanodisks electrodes in Li-ion battery; (d) discharge capacity profile of hexagonal-shaped Co_3O_4 nanodisks electrode as according to cycle numbers.

appears in the FTIR spectrum, if the samples are prepared in the air [16]. A very small absorption band appeared at 1632 cm^{-1} is also observed in the spectrum which is related for bending vibration of absorbed water and surface hydroxyl [16].

Regarding the growth of well-defined Co_3O_4 hexagonal nanodisks, it is important to note that in our experimental conditions only Co_3O_4 hexagonal nanodisks were obtained. However, various reports have been presented in the literature which demonstrated that the size and morphology of Co_3O_4 nanostructures can be controlled by several process factors which include additives, reaction time, precursor, synthesis process and so on. Recently, Choi et al. have reported the synthesis of variety of Co_3O_4 nanostructures using $Co(C_2H_3O_2)_2$ as a precursor of Co and L(+)-lysine monohydrate and oxalic acid as structure directing agents by solvothermal technique [17(a)]. The morphology of the Co_3O_4 nanostructures was controlled by adjusting the concentrations of L(+)-lysine monohydrate and oxalic acid and reaction time. In another report, Patil et al. have reported the growth of Co_3O_4 nanorods using cobalt nitrate and K_2CO_3 via co-precipitation/digestion method by calcination of cobalt hydroxyl carbonate in air at 250 °C [17(b)]. Micelle-assisted hydrothermal synthesis of uniform Co_3O_4 nanorods was done at 180 °C by Teng et al. and reported in the literature [17(c)]. Cao et al. demonstrated a polyol process to synthesize variety of Co_3O_4 nanostructures [17(d)]. They demonstrated that the morphologies of Co_3O_4 can be controllable by tuning the concentration of cobalt precursor and the morphologies of the obtained products varies from simple nanoplates to well-organized cabbage-like structures, and then to microspherical composites [17(d)].

Fig. 3(a) exhibits the typical step-by-step Li-ion battery anode fabrication process using synthesized Co_3O_4 hexagonal nanodisks. The electrochemical performance of Co_3O_4 hexagonal nanodisks as anode was investigated by galvanostatic charge/discharge cycling in the potential range of 0.01 V to 2.5 V *vs.* Li/Li^+ reference electrode. The charge-discharge profile of Li/Co_3O_4 cell is depicted in Fig. 3(b). There are two distinctively clear potential regions: a flat plateau associated with the conversion reactions and a sloping region is ascribed to the formation of a surface layer. A lithium insertion capacity 2039 mAh/g has been achieved during the first lithium insertion. However, only 1147 mAh/g of lithium could be retrieved, which corresponds to a first-cycle irreversible capacity loss of 56%. This loss in capacity is attributed to the formation of Li_2O in the initial conversion reaction as described below:

Lithium insertion process:

$$Co_3O_4 + 8Li^+ + 8e^- \rightarrow 3Co + 4Li_2O \quad (1)$$

Lithium deinsertion (extraction) process:

$$3Co + 4Li_2O \rightarrow Co_3O_4 + 8Li^+ + 8e^- \quad (2)$$

According to Larcher et al. [18] and Fu et al. [19], the active material does not revert to the spinel Co_3O_4 oxide but to the monoxide, CoO. The cycling profile is similar to those reported for nano/micro particles of Co_3O_4 reported earlier [18–20]. In the discharge curve a plateau at around 1.25 V is observed in the first discharge which accounts for about 150 mAh/g of the capacity (or a lithium content of 1.5 per Co_3O_4 molecule). According to Tarascon et al. [21], this plateau appears due to the formation of α-CoO phase which is followed by a long plateau that further substantiates Eq. (1) [18,19]. The sudden voltage drop which falls gradually to the cut-off potential is attributed to the formation of a polymeric surface layer on the electrode particles [22] or to storage of charge/mass at the interface between the Li_2O and Co nanoparticles in the electrode matrix [23]. According to Bruce et al. [20], that the capacities represented by the sloping region did not correspond to surface areas of the electrode material, suggest that the dominant charge storage mechanism is formation of a polymeric surface layer. Fig. 3(d) displays the discharge (de-insertion) capacity as a function of cycle number at room temperature. It may be noted that the materials were cycled well for more than 11 cycles so far. The fade in capacity observed in the present study is much lower than that of Co_3O_4 nanorods reported by Yang et al. [24]. The polymeric elec-

trolyte layer which is supposed to be generated in the first step along with small size of particles in the conversion electrodes help buffer strains during the electrochemical process. It must be noted that the high surface areas presented by the particles facilitate extensive formation of the polymeric surface layer. The small size of the particles (nanodisks) in the conversion electrodes together with the polymeric electrolyte layer supposed to be generated in the first lithiation step help buffer strains during the electrochemical process. The efficient electronic transport provided by the 2D electronic pathway without inter-particle contact resistance and the contribution from the good electrical contact between the nanosheets and current collector offer better cycling performance to the cell. A similar observation has been reported by Kang et al. [25] where the authors reported the cycling behavior of SnS nanosheets.

4. Conclusions

In summary, a facile hydrothermal process was used to synthesize well-defined hexagonal-shaped Co_3O_4 nanodisks at low-temperature of ~110 °C. The detailed morphological and structural characterizations confirmed that the as-grown products are hexagonal-shaped Co_3O_4 nanodisks with internal angle of ~120° and possessing very well crystalline cubic spinel structure. The synthesized nanodisks were used as an anode material for the Li-ion battery applications which exhibited an initial lithium insertion capacity of ~2039 mAh/g and a stable capacity of ~260 mAh/g over 10 cycles. This research exhibits that simply synthesized cobalt oxide nanostructures can efficiently be utilized as an anode material for Li-ion battery applications. However, an intensive research is being carried out to improve the discharge capacity of nanostructured Co_3O_4 and will be communicated in near future.

Acknowledgements

Authors would like to acknowledge the support of the Ministry of Higher Education, Kingdom of Saudi Arabia for this research through a grant for a Collaborative Research Centre on Sensors and Electronic Devices at Najran University, Saudi Arabia, dated 24/3/1432 H, 27/02/2011.

References

[1] Ed.A. Umar, Y.B. Hahn, Metal Oxide Nanostructures and their Applications, American Scientific Publisher, USA, 2010.
[2] (a) D. Fauteax, J. Electrochem. Soc. Proc 94–28 (1994) 379;
(b) P.G. Bruce, B. Scrosati, J.M. Tarascon, Angew. Chem. Int. Ed. 47 (2008) 2930.
[3] (a) M. Armand, J.M. Tarascon, Nature 451 (2008) 652;
(b) L. Tang, M. Salamon, M.R. De Guire, Sci. Adv. Mater. 2 (2010) 79.
[4] (a) M. Winter, J.O. Besenhard, M.E. Spahr, P. Novah, Adv. Mater. 10 (1998) 725;
(b) A.D. Handoko, G.K.L. Goh, Sci. Adv. Mater. 2 (2010) 16.
[5] (a) J.R. Dahn, Phys. Rev. B. 44 (1991) 9170;
(b) D. Vennerberg, Z. Lin, Sci. Adv. Mater. 3 (2011) 26.
[6] Y. Liu, K. Hanai, K. Horikawa, N. Imanishi, A. Hirano, Y. Takeda, Mater. Chem. Phys. 89 (2005) 80.
[7] M.N. Obrovac, L. Christensen, Electrochem. Solid-State Lett. 7 (2004) A93.
[8] K. Wang, X. He, J. Ren, L. Wang, C. Jiang, C. Wan, Electrochim. Acta 52 (2006) 1221.
[9] M. Suzuki, J. Suzuki, K. Sekine, R. Rakamura, J. Power Sources 146 (2005) 464.
[10] X. Wang, X. Chen, L. Gao, H. Zheng, M. Ji, C. Tang, T. Sen, Z. Zhang, J. Mater. Chem. 14 (2004) 905.
[11] W.Y. Li, L.N. Xu, J. Chen, Adv. Funct. Mater. 15 (2005) 851.
[12] Y. Liu, C. Mi, L. Su, X. Zhang, Electrochim. Acta 53 (2008) 2507.
[13] Y. Lu, Y. Wong, Y. Zou, Z. Jiao, B. Zhao, Y. He, M. Wu, Electrochem. Commun. 12 (2010) 101.
[14] T. Ozkaya, A. Baykal, M.S. Toprak, Y. Koseoglu, Z. Durmus, J. Magn. Magn. Mater. 321 (2009) 2145.
[15] S.G. Christokova, M. Stayonava, M. Georgieva, D. Mehandjiev, Mater. Chem. Phys. 60 (1999) 39.
[16] (a) X.M. Liu, X.G. Zhang, S.Y. Fu, Mater. Res. Bull. 41 (2006) 620;
(b) R.A. Nyquist, R.O. Kagel, Infrared Spectra of Inorganic Compounds, Academic Press Inc., New York/London, 1971, p. 220.
[17] (a) K.-I. Choi, H.-R. Kim, K.-M. Kim, D. Liu, G. Cao, J.-H. Lee, Sens. Actuators B 146 (2010) 183;
(b) D. Patil, P. Patil, V. Subramanian, P.A. Joy, H.S. Potdar, Talanta 81 (2010) 37;
(c) F. Teng, W. Yao, Y. Zhu, G. Gao, D.D. Meng, J. Non-Cryst. Solids 355 (2009) 2375;
(d) A.M. Cao, J.S. Hu, H.P. Liang, W.G. Song, L.J. Wan, X.L. He, X.G. Gao, S.H. Xia, J. Phys. Chem. B 110 (2006) 15858.
[18] D. Larcher, G. Sudant, J.B. Lerche, Y. Chabre, J.M. Tarascon, J. Electrochem. Soc. 149 (2002) A234.
[19] Z.W. Fu, Y. Wang, Y. Zhang, Q.Z. Qin, Solid State Ionics 170 (2004) 105.
[20] M. Shaju, F. Jiao, A. Debert, P.G. Bruce, Phys. Chem. Chem. Phys. 9 (2007) 1837.
[21] P. Poizot, S. Laruelle, S. Grugeon, L. Dupont, J.M. Tarascon, Nature 407 (2000) 496.
[22] Z. Yuan, F. Huang, C. Feng, J. Sun, Y. Zhou, Mater. Chem. Phys. 79 (2003) 1.
[23] S. Larulle, S. Grugeon, P. Poizot, M. Dolle, L. Dupont, J.M. Tarascon, J. Electrochem. Soc. 149 (2002) A627.
[24] D. Yang, L. Qi, J. Ma, Adv. Mater. 14 (2002) 1543.
[25] J.G. Kang, J.G. Park, D.W. Kim, Electrochem. Commun. 12 (2010) 307.